Determination of Horn Antenna Phase Centers by Edge Diffraction Theory

MARTIN TEICHMAN, Member, IEEE
IBM Corporation
Gaithersburg, Md. 20760

Abstract

The edge diffraction method of analysis utilized in the past to determine amplitude patterns is extended in this paper to predict the radiation phase center of pyramidal horn antennas. A series of extensive phase and amplitude measurements were performed on these antennas to determine the validity of the theoretical results. The measurements were performed over a frequency range of 7.5 to 10.5 GHz in the E plane of the antennas. The phase measurements were accurate to ± 0.2 electrical degrees, so that the phase center locations relative to the horn apertures were repeatably determined to better than 0.010 inch for horn apertures as large as 7 inches.

The results of the measurements indicate that excellent agreement is obtained with the theory in predicting the phase center location of the larger horns ($kRE > 50$). For the smaller horns, however, there is a large discrepancy between the theory and measurements. The measured phase centers of the smaller horns exhibit a large variation with frequency which cannot be explained with the existing theory. Several reasons for the discrepancy are presented, and it is concluded that a more rigorous approach involving higher order modes has to be developed for the smaller horns.

Manuscript received April 20, 1973.

List of Symbols

A = field amplitude
α = E-plane flare angle
a = E-plane waveguide dimension
β = H-plane flare angle
b = H-plane waveguide dimension
DE = E-plane aperture dimension
DH = H-plane aperture dimension
E_F = far-field electric field intensity
$k = 2\pi/\lambda$ = wave number, phase constant
λ = wavelength
RE = E-plane slant height
RH = H-plane slant height
Φ = far-field phase function
Ψ_A = aperture field phase function
r, θ, φ = variables, spherical coordinates
x, y, z = variables, rectangular coordinates
n = wedge angle function where $(2-n)\pi$ = wedge angle
V_B = edge diffracted field intensity
Ψ_r = angle from edge to field point
Ψ_0 = angle from edge to source point
Δ = phase center distance as measured from aperture.

I. Introduction

In such applications as precision direction finding systems, monopulse systems, and high resolution interferometer systems, it is necessary to accurately determine the phase center of the radiating element. In addition, knowledge of the location of the phase center is necessary for the successful design of phased-array antennas and primary feeds for reflectors. The phase center of a radiating element can be defined by considering the element as an equivalent point source within a certain angular region about the main lobe of radiation. This is valid only if the equiphase surfaces of the far-field radiation are concentric spheres in this region. The phase center of these concentric equiphase spheres is defined as the phase center of the radiating element. If the locus of phase centers in all planes is a point, then the radiation seems to emanate from a point source. In general, this locus of phase centers does not result in a point in space, but is a line, circle, or other shape. The phase center, therefore, is uniquely defined only in a particular plane and only over a specified field of view.

A number of workers have considered this problem in the past. Morita [1] analyzed the phase characteristics of monopole antennas and presented measurements to determine the phase center. The accuracy of his system was only about 3 degrees, so that precise phase center locations were not obtained; however, general trends were observed. Reid [2] presented some phase center results which were determined by amplitude measurements. The results obtained for sectoral horn antennas are very inconclusive, since only two antennas were measured and no patterns were presented.

Cheng [3] presented theoretical and measured results for the phase centers of helical beam antennas. He concluded that the theoretical and measured phase results did not agree closely. Barbano [4] presented measured results for spiral antennas. Again, close agreement between the theory and measurements was not obtained, although a general trend was observed. Carter [5] presented an analysis for the phase center of parabolic antennas, although no measurements were included. Hu [6], Muehldorf [7], and Baur [8] presented theoretical results for the determination of horn phase centers, but no measurements were included.

This paper presents the results of extensive phase and amplitude measurements of pyramidal horn antennas in order to determine the phase center location. The measurements were made at X band over a frequency range of 7.5 to 10.5 GHz in both the E and H planes. In the past, phase measurements were very difficult and usually inaccurate. Utilizing the techniques presented in this paper, the phase measurements are accurate to ±0.2 electrical degree, so that the phase center can be repeatably determined to better than 0.010 inch.

The edge diffraction method, utilized in [9] to determine horn amplitude patterns, is here extended to predict the phase centers. Although measurements were made in both E and H planes, only the former results are presented because of the similarity in the results obtained and to limit the size of this paper.

Section II presents the theoretical analysis, and Section III describes the measurement setup and the results of the measurements. Typical measured patterns are also included. Section IV presents a discussion of the results and conclusions.

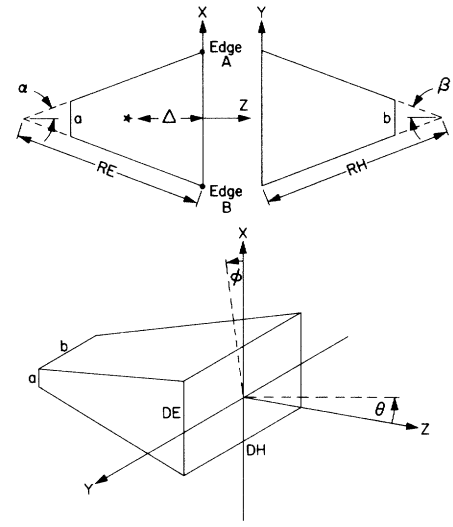

Fig. 1. Horn and coordinate geometry.

Fig. 2. Diffraction from a wedge.

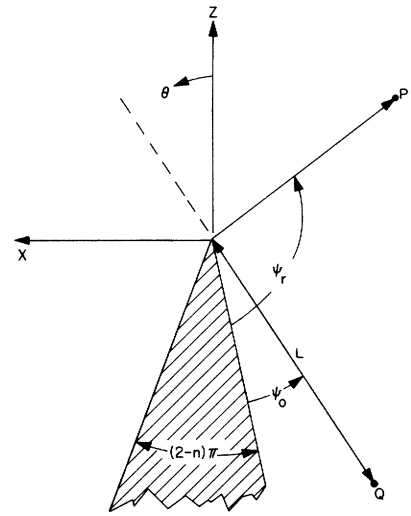

II. Theoretical Determination of the Phase Center

The phase center of an antenna can be defined as the reference point from which the far-field radiation seems to emanate. Criteria on the antenna excitation for the existence of a unique phase center have been established [10] and the location of this point, if it exists, can be analytically determined for any radiating structure for which the radiated field expression is known. In general, such a point can be established over a narrow angular region of space within the −3-dB beamwidth of the antenna [6]. To determine this point, the far-field phase variation must first be determined. In this section, the far field of a pyramidal horn antenna is determined by means of edge diffraction theory.

The edge diffraction method considers the diffraction by a conducting wedge. The resulting radiated field may be treated as a superposition of the geometrical optics field and the diffracted field from the antenna edges. Thus, the techniques of ray optics can be used, and the radiated field can be determined from the edge diffracted rays and the geometrical optics rays.

Edge diffraction expressions were first derived by Sommerfeld [11] and simplified by Pauli [12]. Amplitude patterns of horn antennas by this method were derived by Kinber [13] and Rudduck [9], [14]. For a pyramidal horn, the E- and H-plane patterns are determined mainly by diffraction from the E-plane edges (the edges located in the Y-Z plane of Fig. 1), since the field goes to zero at the H-plane edges (the edges located in the X-Y plane). The H-plane pattern is determined by considering the diffraction along the entire length of the E-plane edge. The E-plane pattern is determined by diffraction from the midpoints of the edges. In this section, only the E-plane phase patterns are derived.

The antenna model is a corner reflector formed by two perfectly conducting plane walls intersecting at an angle 2α. To simplify the analysis, the reflector is assumed to be infinite in the Y direction, thus reducing the problem to a two-dimensional analysis. In this analysis, only the first-order diffraction terms are presented, since it was determined that the higher order terms involving multiple edge

diffraction contribute negligibly to the main lobe region and, therefore, do not influence the phase center location. The first-order terms include the direct radiation of the primary source S (a line source at the apex) and the diffraction from edges A and B when illuminated by S.

In this analysis, the diffraction of a cylindrical wave by a perfectly conducting wedge is employed. Considering the wedge shown in Fig. 2, the far-field edge diffracted signal induced by an incident cylindrical wave may be expressed as (where the radial distribution of the line source and diffracted signals $e^{-jkr}/\sqrt{r}$ is assumed)

$$U = V_B(L, \Psi_r - \Psi_0, n) \pm V_B(L, \Psi_r + \Psi_0, n) \tag{1}$$

where

$$V_B(L, \Psi, n) = \exp\left[j\left(\frac{\pi}{4} + kL\cos\Psi\right)\right] \cdot \frac{2\left|\cos\frac{\Psi}{2}\right| \sin\frac{\pi}{n}}{\sqrt{\pi}\, n\left(\cos\frac{\pi}{n} - \cos\frac{\Psi}{n}\right)} \cdot \int_{\sqrt{akL}}^{\infty} e^{-j\tau^2}\, d\tau + \text{higher order terms} \tag{2}$$

and $a = (1 + \cos\Psi)$ and $(2 - n)\pi$ = the wedge angle.

The higher order terms are usually small, except when kL is small, and are identical to zero for $n = 2$. The positive sign applies for the electric field polarization perpendicular to the edge, while the negative sign is for the electric field polarization parallel to the edge. The phase reference for this formulation is at the edge; the superposition of diffraction from several edges required the use of a common phase reference. The common phase reference is here taken at the center of the horn aperture.

Using the notation of [9], the first-order diffraction terms are as follows.

1) The direct radiation of the source is expressed as v^*, where

$$v^* = \begin{cases} 1, & |\theta| < \alpha \\ 0, & |\theta| > \alpha \end{cases}. \tag{3}$$

The direct source illuminates only in the forward region, and is zero in the shadow region.

2) The diffraction from edge A of wedge angle $(2 - n)\pi = 0$, illuminated by a source at the apex, is D_{AS}. The distance from the source to the edge is the slant height of the horn, RE, and the angle to the field point is $\pi - \alpha + \theta$. Therefore,

$$D_{AS} = V_B(RE, \pi - \alpha + \theta, 2). \tag{4}$$

3) The diffraction from edge B when illuminated from the source at the apex is, similarly,

$$D_{BS} = V_B(RE, \pi - \alpha - \theta, 2) \tag{5}$$

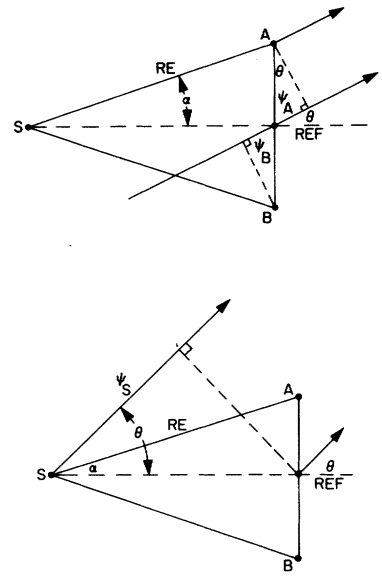

Fig. 3. Phase relationships at horn edges.

where the reflected terms involving $\Psi + \Psi_0$ are eliminated at grazing incidence $\psi_0 = 0$.

Term b is valid in the region

$$-\frac{\pi}{2} \leqslant \theta \leqslant \pi + \alpha$$

and is zero elsewhere, since it is blocked by the wall of B. Similarly, term c is valid in the region

$$-(\pi + \alpha) \leqslant \theta \leqslant \frac{\pi}{2}$$

and is zero elsewhere, where it is blocked by the wall of A.

If we let the phase reference be at the center of the aperture, the phase at points A and B referred to the reference can be determined from Fig. 3 as

$$Y_A = \exp\left(j\,\frac{kDE\sin\theta}{2}\right)$$

$$Y_B = \exp\left(-j\left|\frac{kDE\sin\theta}{2}\right.\right).$$

The phase of the line source referred to the midpoint is simply

$$Y_S = \exp(-jkRE\cos\alpha\cos\theta).$$

The total radiated field is therefore

$$E_{F1} = (Y_S \times v^*) + (D_{AS} \times Y_A) + (D_{BS} \times Y_B). \tag{6}$$

This expression was resolved into real and imaginary components and numerically evaluated by computer to determine the amplitude and phase of the radiation pattern.

The phase center can now easily be determined from the theoretical phase patterns. Using the method of [6], the phase center is determined graphically from the slope of the phase term versus $\cos\theta$. The linear portion of the curve determines the valid region for the existence of the phase

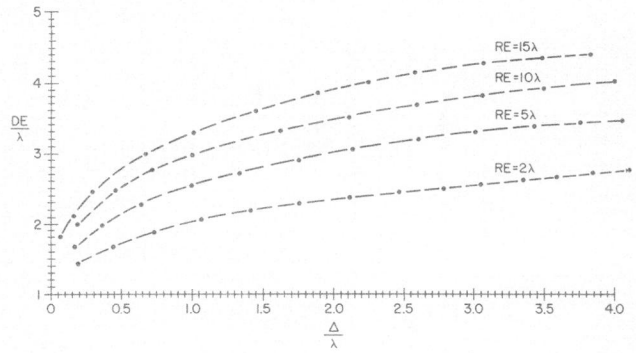

Fig. 4. *E*-plane phase center of pyramidal horn.

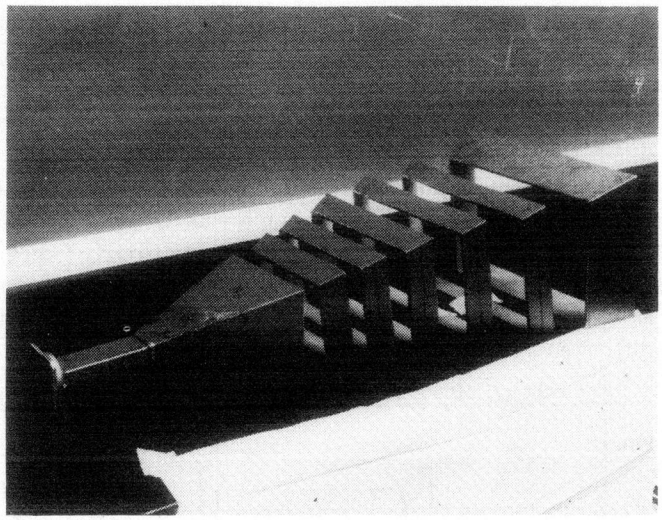

Fig. 5. Test horn.

center, and the slope determines the phase center. This results from postulating that there is a phase center located on the axis of symmetry a distance Δ from the origin. The spherical radiation field emanating from a point source at the phase center can be written as

$$E_F = A \exp\left[-jk(r + \Delta \cos\theta)\right].$$

Comparing this expression to the general far-field expression $E_F = A \exp -j[kr + \Phi]$, the phase center location is determined from

$$\Delta = \frac{\Phi}{k \cos\theta}. \tag{7}$$

The results of the phase center analysis are presented in Fig. 4. For very small horns, the phase center approaches the aperture as it does for an open-ended waveguide. For large horns, the phase center moves away from the aperture. It should be noted that these results are almost identical to the results obtained by Muehldorf [7] using conventional aperture theory. This proves the extreme utility of the edge diffraction method as opposed to the more cumbersome aperture method. In addition, the former method can easily be extended to include the effects of ground planes and other structures around the horn, while the latter cannot.

TABLE I

Test Horn Dimensions

$\alpha = 12° 41'$, $a = 0.400$ inch
$\beta = 16° 11'$ $b = 0.900$ inch

Horn	*DE* (inch)	*DH* (inch)	*RE* (inch)	*RH* (inch)
1	5.67	7.70	12.9	13.8
2	4.77	6.44	10.8	11.5
3	4.30	5.95	9.8	10.6
4	3.90	5.39	8.9	9.7
5	3.43	4.80	7.8	8.6
6	3.05	4.23	6.9	7.6
7	2.58	3.68	5.9	6.6

Relationships for physically realizable horn:

$$\frac{DE - a}{2 \tan\alpha} = \frac{DH - b}{2 \tan\beta}$$

$$\sin\alpha = \frac{DE}{2RE}, \quad \sin\beta = \frac{DH}{2RH}.$$

III. Phase Center Measurements

To ascertain the validity of the theoretical analysis, several phase measurements were conducted to determine the phase center of pyramidal horns of varying dimensions. To conveniently obtain several horn cross sections, it was decided to utilize an *X*-band standard gain horn the aperture of which was successively reduced by shearing off increments along the axis of the horn. Fig. 5 shows the test horn and indicates the sections that were removed. The aperture dimensions and the horn lengths are tabulated in Table I. Using this technique, several aperture sizes and lengths were obtained with a single horn of constant flare angle. In addition, the measurements were made over a frequency range of 7.5 to 10.0 GHz in order to assess the effects of frequency variations on the phase center. The measurements were mainly performed in the *E* plane, with some *H*-plane measurements included for completeness. Only the former results are presented here for conciseness.

The measurements were performed in a tapered anechoic chamber approximately 280 inches long. The chamber was checked out to determine the magnitude of the spurious reflections. The results indicated that at *X* band the average reflected signal level was 55-dB below the incident signal in a 40 inch by 40 inch test area. This is an important factor, since reflections can cause amplitude and phase errors in the measurements. For the reflection levels measured, an uncertainty of less than ±0.2 electrical degrees, which is negligible for these measurements, is introduced.

The antenna was mounted on a cross-slide fixture attached to a Scientific Atlanta rotary pedestal. The cross slide is of the type normally utilized for milling machine operations. It allows the antenna to be positioned along mutually perpendicular axes, along and perpendicular to

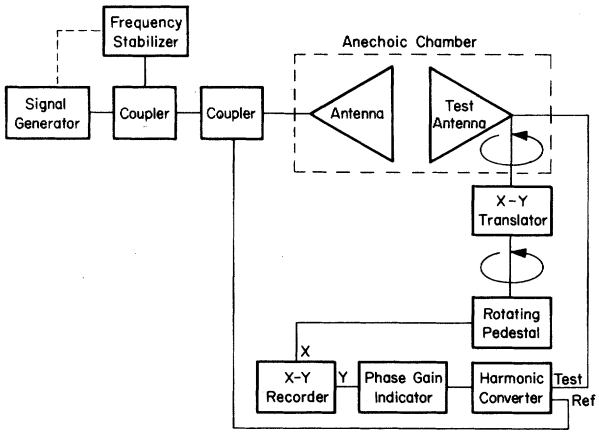

Fig. 6. Measurement setup for determination of horn phase center.

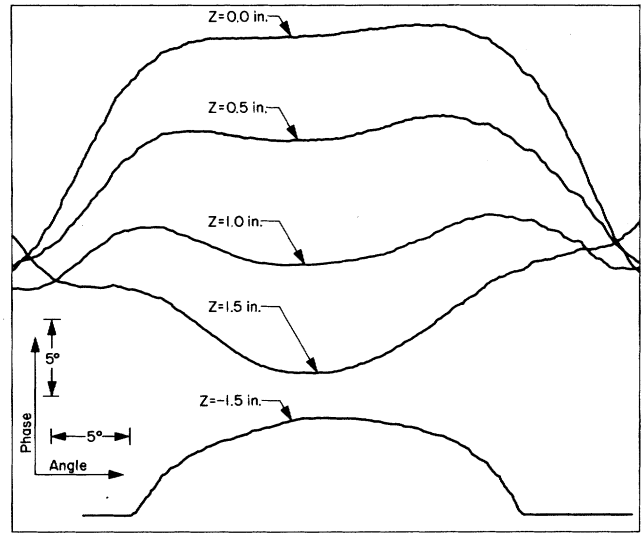

Fig. 7. Variation of measured phase pattern.

the chamber axis, in increments of 0.001 inch. An airline rotary joint was mounted in the center of the pedestal so that connections could be made to the antenna without incurring any cable flexing during the measurements. Such cable flexing can introduce serious phase errors. The test antenna was illuminated from the tapered end of the chamber by a horn antenna. The received signal at the test antenna was compared with the transmitted reference signal in both amplitude and phase.

The instrument utilized as the phase/amplitude measuring unit was the Hewlett-Packard network analyzer, model 8410 [15]. This instrument is capable of performing phase comparison at X band to within ±0.1 electrical degree accuracy. The dc output of the analyzer was fed into an X-Y recorder, where the patterns were recorded. The transmitter frequency was stabilized using an external phase-locked loop, so that any phase errors caused by frequency drift were eliminated. A block diagram of the measurement setup is presented in Fig. 6.

The measurement of phase patterns and phase centers at X band places stringent requirements on the antenna mounting equipment. The minimum physical requirement of the equipment is the ability to rotate a selected position on the antenna about a point in space, i.e., the center of rotation of the pedestal. Movement of this position on the antenna (caused by pedestal vibration or other factors) by, for example, 0.010 inch can cause a 3 degree phase error. For accurate phase measurements, it is also necessary to properly align the antenna so that repeatable measurements can be performed. To accomplish these aims, the antenna was mounted and aligned using optical techniques. The Keuffel and Esser (K & E) leveling telescope, a precision collimating mirror, and several targets were used. A complete description of this technique can be found in [16].

For most antennas, an apparent phase center can be determined over a specified portion of space. This center acts as the apparent source of the antenna radiation. In general, the phase center position is different for the E and H planes and for any plane in between. When the antenna is positioned so that the phase center is directly over the antenna axis of rotation, the phase pattern in the far field will be constant over the portion of space for which the phase center is defined. If the horn is made perfectly symmetrical, the phase centers will lie on the horn axis. However, because of practical tolerance limitations, the horn is usually not perfectly symmetrical. The phase centers are actually removed from the mechanical axis of the horn depending on the symmetry and orthogonality of the horn sides. The effects on the horn phase patterns of a phase center displaced from the axis of rotation can be determined from simple geometrical considerations.

Let the phase center be located at a point in space (x_0, y_0, z_0) where the origin of the coordinates is the center of antenna rotation. If we assume that the observation point is on the z axis at $(z_1, 0, 0)$, and the distance to the phase center is d_0, then

$$d_0 = \sqrt{(z_1 - \rho\cos\phi\cos\theta)^2 + \rho^2\cos^2\phi\sin^2\theta + \rho^2\cos^2\phi} \approx z_1 - \rho\cos\phi\cos\theta \quad \text{for } z_1 >> \rho \quad \text{(far field)}. \quad (7)$$

If the initial phase reference is at the boresight of the antenna, then

$$d_0 = z_1 - \rho\cos\varphi\cos\theta_0.$$

As the phase center rotates about the axis of rotation (φ = constant), the phase change caused by the change in d is given by

$$\frac{2\pi}{\lambda}(d - d_0) = \frac{2\pi}{\lambda}\rho\cos\varphi[\cos\theta_0 - \cos(\theta_0 + \theta)]$$

$$= \frac{2\pi}{\lambda}r[\cos\theta_0 - \cos(\theta_0 + \theta)]. \quad (8)$$

The shape of the phase patterns indicates the phase center position relative to the center of rotation. Fig. 7 presents typical measured phase patterns indicating these variations.

The following observations can be made from the measured phase patterns when the phase center is not aligned with the center of rotation:

1) If the phase center lies on the axis of the antenna (the z axis), then a symmetrical phase pattern results. Any motion along this axis will produce flatter phase patterns as the center of rotation is approached. If the center of rotation is passed, the phase patterns will again be curved, but this time the curve will be of the opposite slope (see Fig. 7).

2) If the phase center is moved off the z axis, the phase pattern will be asymmetrical. Motion along the z axis will now cause a successive change in slope as the phase center passes through the center of rotation.

In theory, the phase center can be determined from one phase pattern. If a change in phase is measured as the antenna is rotated from $\theta = 0$ degrees to $\theta = \theta_1$, the phase center is displaced from the center of rotation a distance of

$$r = \frac{\lambda}{2\pi} \frac{\delta\Phi}{1 - \cos\theta_1}$$

where $\delta\Phi$ is the measured phase difference from $\theta = 0$ degrees to $\theta = \theta_1$. It is evident that as r decreases, the change in phase decreases. Thus, the resolution of the phase measuring equipment limits the accuracy of the phase center determination. For these measurements, the minimum resolution was 0.1 degree. If the phase center is defined over 30 degrees, the minimum detectable phase center position at 7.5 GHz is therefore $r = 0.008$ inch. For the horns with narrow beamwidths (1, 2, and 3), the phase center is defined over about 10 degrees, so that the minimum detectable distance is $r = 0.030$ inch. In this instance, the phase center can be more accurately determined by an averaging technique. Thus, the antenna is positioned so that the phase center is first behind, then in front, of the center of rotation in equal increments, resulting in symmetrical patterns of opposite concavity. The phase center is then located halfway between these two positions.

The results of the phase center measurements are summarized in Fig. 8 for horns 1 through 4 and in Fig. 9 for horns 5 through 7. The theoretical results using edge diffraction are shown for comparison. Some interesting observations can be made from Figs. 8 and 9. The measured results agree quite well with the calculated results for horns 1 and 2 over the frequency band and partially for 3 and 4 at the higher frequencies. These are the larger horns. The measurements, however, depart quite drastically from the predicted results for horns 5 through 7, the smaller horns. Whereas the theory predicts a smooth curve versus frequency, the measurements indicate wide variations in phase center location. The next section presents a further discussion of these results.

For the horns for which good agreement between theory and measurements is obtained, the agreement is excellent in both the amplitude and phase patterns. Figs. 10 and 11 show typical measured E-plane amplitude and phase patterns for horns 1 and 2, respectively. The theoretical results are shown for comparison. Note the excellent agreement in both amplitude and phase over the entire field of view. This excellent agreement indicates the validity of the simple edge diffraction analysis, at least for the larger horns.

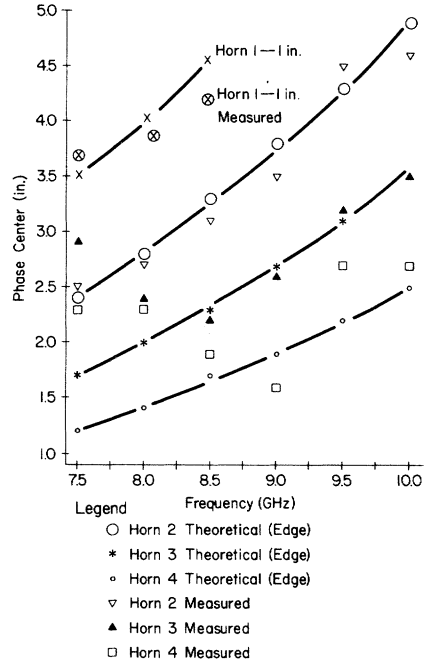

Fig. 8. Variation of phase center with frequency (horns 1 through 4).

Fig. 9. Variation of phase center with frequency (horns 5 through 7).

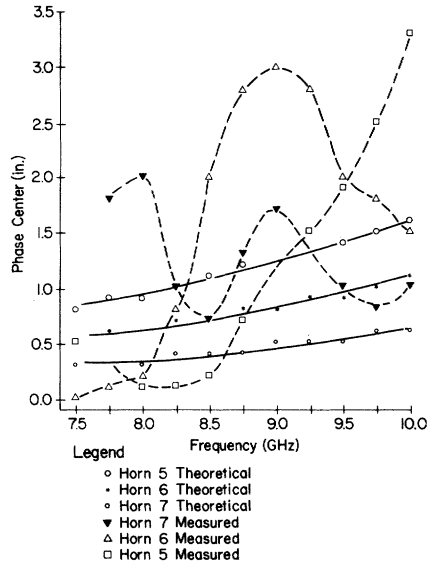

IV. Conclusions

This paper has presented the results of an extensive series of phase and amplitude measurements of pyramidal

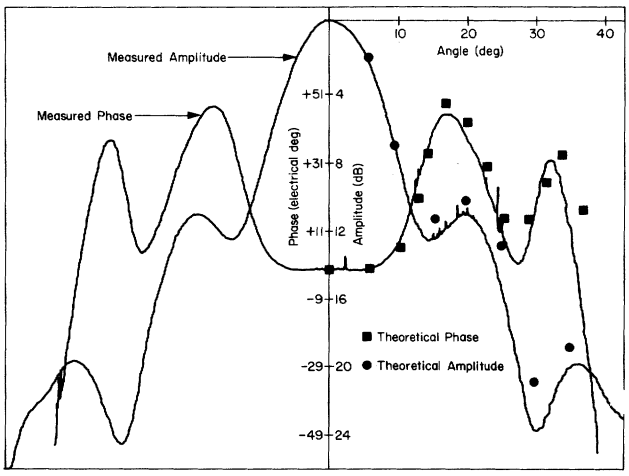

Fig. 10. Typical amplitude and phase patterns (*E*-plane; horn 1).

Fig. 11. Typical amplitude and phase patterns (*E*-plane; horn 2).

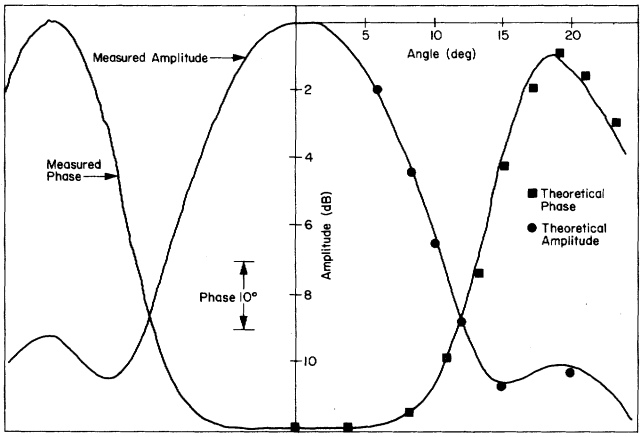

horn antennas. The purpose of the measurements was to determine the phase center properties of these horns. The measurements indicate surprising results which have not been previously presented in the literature.

As can be seen in Figs. 8 and 9, the phase center location of a pyramidal horn is a well-behaved function versus frequency for the larger horns ($kRE > 50$). However, the phase variation is quite drastic over the same frequency range for the smaller horns. Conventional aperture theory presented in [7] does not predict this type of behavior. It was at first suspected that edge diffraction theory would predict such variations; however, the results obtained were very similar to the aperture method. It is interesting to note in this respect that the simple edge diffraction theory can accurately determine the phase and amplitude patterns of the larger horns. This proves the extreme utility of this method as opposed to the more cumbersome aperture method. In addition, the edge diffraction method can easily be extended to include such effects as thick horn walls and horns mounted in a finite ground plane, while the aperture method cannot.

Although the measurements and theory differed widely for the smaller horns, they agreed quite closely for the larger horns. This is noteworthy, since the theoretical analysis includes approximations which are generally valid for large horns (in terms of wavelengths). The measured results seem to deviate at the lower frequencies first, where, in essence, the horn is smallest in wavelength. Several possible reasons can be presented to explain the discrepancy for the smaller horns. One explanation is that the theoretical analysis fails to take into account any higher order modes introduced at the throat of the horn. For the larger horns, these higher order modes are attenuated to a negligible amplitude before reaching the aperture. However, for the shorter horns, these fields may not have sufficiently decayed, and it may be necessary to take them into account.

A second possible explanation is inherent in one of the assumptions made in the theoretical analysis. It is assumed that the radiation source is at the apex of the horn and that a wave with a cylindrical phase front radiates towards the aperture. This is a good approximation for the larger horns, since the aperture is far from the apex, thus allowing ample wavelengths for the phase front to develop. However, for shorter horns, since the apex is close to the aperture, the wave phase front may not be cylindrical.

Finally, reflection interactions occur within the horn between the throat and the aperture discontinuities. In the longer horns this interaction can be neglected, but, because of the close proximity between the aperture and throat in the shorter horns, it cannot be neglected. The result is a different field distribution in the horn than that assumed. In general, all these effects would be sensitive to frequency, as was observed. Since these effects are small, they would tend to influence the phase patterns much more than the amplitude patterns, and, hence, the phase center itself.

The results of this paper indicate that close agreement between measured and predicted results can be obtained for long horns ($kRE > 50$) using simple edge diffraction theory. The results are extremely accurate in both the amplitude and phase patterns, and thus also in the determination of the phase center. For the smaller horns, the theory is inadequate to predict the measured results. Several effects have been considered to explain this discrepancy; however, the theoretical analysis then becomes difficult or impossible.

Acknowledgments

The author is indebted to Prof. B. Senitzky, thesis adviser, for his encouragement and assistance. The author also acknowledges the suggestions of and helpful discussions with E. Kramer, H. Yin, and E. Muehldorf during the preparation of this paper. Special thanks is accorded to A. Parr for his assistance in performing the numerous measurements, and to F. Marek for his assistance in preparing the computer programs.

References

[1] T. Morita, "Determination of phase centers and amplitude characteristics of radiating structures," Stanford Research Inst., Calif., Tech. Rept. I, SRI Project 898, March 1955.

[2] R. Reid, Jr., "Determination of phase center location by amplitude measurements," Syracuse University Research Inst., Syracuse, N.Y., Rept. EE492-6008T10, August 1960.

[3] D.K. Cheng and S. Sander, "Phase center of helical beam antennas," *1958 IRE Natl. Conv. Rec.* pt. I, pp. 152-157.

[4] N. Barbano, "Phase center distributions of spiral antennas," *IRE Wescon* pt. I, pp. 132-130, August 1960.

[5] D. Carter, "Phase centers of microwave antennas," *IRE Trans. Antennas and Propagation*, vol. AP-4, pp. 597-600, October 1956.

[6] Y.Y. Hu, "A method of determining phase centers, and its application to electromagnetic horns," *J. Franklin Inst.*, pp. 31-39, January 1961.

[7] E.I. Muehldorf, "The phase center of horn antennas," *IEEE Trans. Antennas and Propagation*, vol. AP-18, pp. 753-760, November 1970.

[8] K. Baur, "The phase center of aperture radiators," *Arch. Elekt. Ubertragung*, vol. 9, pp. 541-546, 1955.

[9] J.S. Yu, R.C. Rudduck, and L. Peters, Jr., "Comprehensive analysis for *E*-plane of horn antennas by edge diffraction theory," *IEEE Trans. Antennas and Propagation*, vol. AP-14, pp. 138-149, March 1966.

[10] A.R. Vol-pert, "The notion of a phase centre in aerial design" (transl.), *Radio Engrg. Electron. Phys.* (USSR), vol. 16, no. 3, 1961.

[11] A. Somerfeld, *Optics.* New York: Academic Press, 1954, pp. 254-265.

[12] W. Pauli, "On asymptotic series for functions in the theory of diffraction of light," *Phys. Rev.*, vol. 54, pp. 924-931, December 1938.

[13] B. Ye Kinber, "Diffraction at the open end of a sectoral horn" (transl.), *Radio Engrg. Electron Phys.* (USSR), vol. 7-10, pp. 1620-1632, October 1962.

[14] P.M. Russo, R.C. Rudduck, and L. Peters, Jr., "A method of computing *E*-plane patterns of horn antennas," *IEEE Trans. Antennas and Propagation*, vol. AP-11, pp. 219-224, March 1965.

[15] "An advanced new network analyzer for sweep-measuring amplitude and phase from 0.1 to 12.4 GHz," *Hewlett-Packard J.*, pp. 2, February 1967.

[16] M.A. Teichman, "Precision phase center measurements of horn antennas," *IEEE Trans. Antennas and Propagation*, vol. AP-18, September 1970.

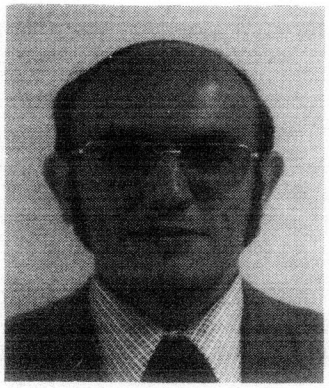

Martin A. Teichman (S'63–M'68) received the B.E.E. degree from the City College of New York, N.Y., in 1965 and the M.E.E. degree from the Polytechnic Institute of Brooklyn, N.Y., in 1970.

From 1965 to 1967 he was a member of the staff at Wheeler Laboratories, Smithtown, N.Y., where he helped develop techniques for the simulation of phased arrays in triangular and rhombic waveguides. He designed several IFF arrays and developed methods for successfully integrating IFF and radar antennas into single dual-frequency radomes. He also participated in the development of an array element for the Missile Site radar, and several personnel protection fences that were installed around the radar, at White Sands, N. Mex. He has been with IBM Corporation since 1967. From 1967 to 1969 he participated in the development of Gunn and LSA oscillators for microwave applications as part of the IBM Center for Exploratory Studies at Yorktown Heights, N.Y. He also participated in the design of a singing retrodirective array for Rome Air Development Center. Since 1969 he has been involved in the design, development, and implementation of an RF interferometer for the ATS-F satellite, at IBM, Gaithersburg, Md.

Mr. Teichman is a member of Eta Kappa Nu.